Antibubble Dynamics: The Drainage of an Air Film with Viscous Interfaces

Benoit Scheid,[1] Stéphane Dorbolo,[2] Laura R. Arriaga,[3] and Emmanuelle Rio[3]

[1]*TIPs, Université Libre de Bruxelles C.P. 165/67, 1050 Brussels, Belgium, EU*
[2]*GRASP, Physics Department B5, Université de Liège, 4000 Liège, Belgium, EU*
[3]*LPS-UMR8502, Université Paris-Sud, 91405 Orsay, France, EU*

An antibubble is a spherical air film that is immersed in a surfactant mixture and drains under the action of hydrostatic pressure. A dynamical model of this film is proposed that accounts for the surface shear viscosity effects in the case of purely viscous interfaces, which applies for surfactants whose adsorption rate is much larger than advection rate and at a concentration much above the critical micelle concentration. Our model shows that the lifetime of the antibubbles in this case increases with surface shear viscosity, denoted ε, whose value is measured independently, all in agreement with experimental measurements. We also found that the critical thickness, h_c, at film rupture due to van der Waals interactions slightly depends on the surface shear viscosity, namely $h_c \propto \varepsilon^{1/6}$.

Foams are often used under various flow regimes, whose specific applications in technological processes rely essentially on their properties. Among these, the surface rheological properties are probably today the most challenging ones to be modeled (see, e.g., Ref. [1]). In foam dynamics as in most of dynamical systems involving fluid-fluid interfaces with surface-active materials, like in coalescence processes, both surface viscosity and elasticity, with both shear and dilational components, are often indissociable, which makes the physical interpretation difficult, if not impossible. Still for some specific flow situations with an appropriate surfactant mixture, conditions can be reached where only one component dominates the others [2]. The claim of the present Letter is that such a situation can be met with antibubbles.

An antibubble is a centimetric spherical air shell surrounded by liquid (see, e.g., Ref. [3]). The antibubble differs from the soap bubble for two main reasons. First, there exists no electrostatic repulsion force that stabilizes the film of air [4], making the antibubble an ephemeral object in which the air drains against gravity due to the hydrostatic pressure gradient, until the film breaks down. Secondly, the effect of confinement [5] responsible for the Marangoni effect that opposes to drainage in soap films is absent in antibubbles because surfactant molecules are in the continuous phase and not in the film. Consequently the drainage of antibubbles essentially depends on surface viscosity, which makes the object unique in exploring the field of surface rheology. This is supported by the overestimation of antibubble lifetimes when modeling the antibubble dynamics with immobile interfaces [3].

Due to the spherical nature of the air flow going from the south to the north poles, interfacial velocity gradients are undoubtedly present, which suggests that the surface density of surfactants varies with position along the interface. However, if the time τ_{ads} for surfactant molecules to adsorb

at the interface is much shorter than the time τ_{adv} for these molecules to be advected by the interfacial flow, the surface density of the surfactant can be assumed to be uniform. The aim of the present Letter is to demonstrate that assuming purely viscous interfaces allows us to rationalize lifetime measurements of antibubbles made with surfactant mixtures that have fast adsorption kinetics and sufficiently high surface shear viscosity, denoted ε, whose value is measured independently.

We model an antibubble as a spherical air film of radius R surrounded by liquid (see Fig. 1). The interfaces are assumed to be material, i.e., we neglect gas absorption against which the surfactant monolayer causes an interfacial resistance [6]. As in soap bubbles, the sphericity of the inner interface is ensured by the excess of Laplace pressure $2\gamma/R$ in the inner liquid, where γ is the surface tension. The position of the inner interface of the film is therefore fixed at $r' = R$, while the position of the outer interface is defined at $r' = R + h(t, \theta)$, where h is the film thickness
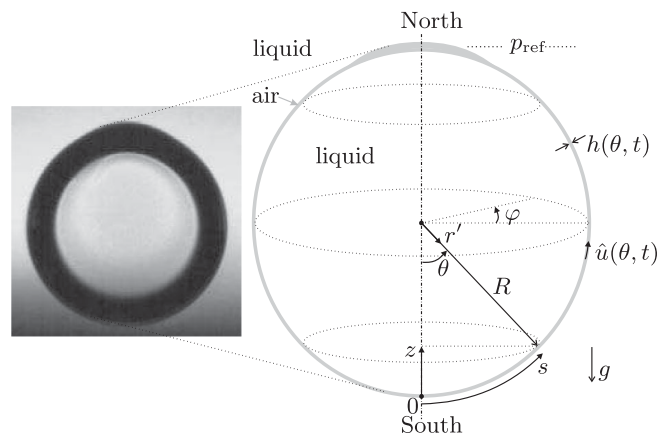

FIG. 1. Picture and sketch of the antibubble with $R \sim 1$ cm, $h \sim 1$ μm (the large black stripe is due to total reflection).
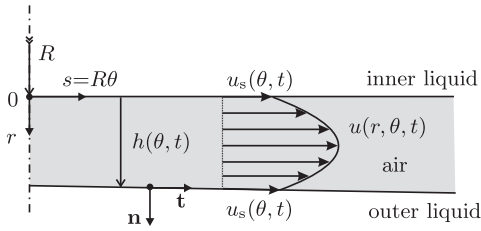
FIG. 2.   Details of the flow in the air film with nearly parallel
interfaces, the thickness h increasing with θ due to drainage.

(see Fig. 2), which depends on time t and on the polar
coordinate $\theta \in [0, \pi]$, or alternatively the curvilinear
coordinate $s = R\theta$, that has its origin at the south pole.
The system is also considered to be symmetric around the z
axis, i.e., uniform in the azimuthal direction φ.

The air in the film is assumed to be incompressible
and flows against gravity due to the hydrostatic pressure
difference between the poles, namely $p_0 = 2\rho g R$, where ρ
is the liquid density and g the gravitational acceleration.
With time, the air thus accumulates at the north pole, as
shown in Fig. 1. Defining the time scale for drainage $\tau =
\mu_{\mathrm{air}}\pi^2 R/(\rho g h_0^2)$ as well as the velocity scale $u_0 = \pi R/\tau$,
where μ_{air} is the dynamic viscosity of air and h_0 corre-
sponds to the average initial thickness, the dimensionless
variables can be rewritten as $h = h_0\bar{h}$, $t = \tau\bar{t}$, $\theta = \pi\bar{\theta}$,
$u = u_0\bar{u}$, and $p = p_0\bar{p}$, where the bar denotes a dimen-
sionless variable. Because the film thickness is of micron
scale [7], the smallness of the aspect ratio $h_0/(\pi R) \sim 10^{-4}$
allows us to write the balance equations in the frame of the
lubrication theory, in which the conservation equation has
the form (see derivation in Ref. [8]):

$$\frac{\partial \bar{h}}{\partial \bar{t}} + \frac{1}{\sin(\pi\bar{\theta})} \frac{\partial}{\partial \bar{\theta}}\left[\bar{h}\sin(\pi\bar{\theta})\left(\bar{u}_s - \frac{\bar{h}^2}{6}\frac{\partial \bar{p}}{\partial \bar{\theta}}\right)\right] = 0. \quad (1)$$

The most general linear relation between the surface stress
tensor and the surface rate of deformation tensor, which
has received must attention in the literature, is the linear
Boussinesq-Scriven surface fluid model [9]. This model
is the surface analog of the bulk stress-strain relationship
of a given fluid. Consequently, as for an incompressible
fluid, only the shear component remains for an interface
with constant surfactant density, as assumed in this work.
Considering further that the surface shear viscosity ε
remains constant, say for a "Newtonian" interface, the
Boussinesq-Scriven model yields, respectively, to the fol-
lowing form of the normal and tangential stress boundary
conditions (see derivation in Ref. [8]):

$$\frac{\partial \bar{p}}{\partial \bar{\theta}} = \frac{1}{2}\frac{\partial}{\partial \bar{\theta}}\left[\cos(\pi\bar{\theta}) - \frac{\mathrm{Bo}}{\sin(\pi\bar{\theta})}\frac{\partial}{\partial \bar{\theta}}\left(\sin(\pi\bar{\theta})\frac{\partial \bar{h}}{\partial \bar{\theta}}\right) + \frac{A}{\bar{h}^3}\right],$$
$$(2)$$

$$\bar{h}\frac{\partial \bar{p}}{\partial \bar{\theta}} = 2\mathrm{Bq}\left[\frac{\partial}{\partial \bar{\theta}}\left(\frac{1}{\sin(\pi\bar{\theta})}\frac{\partial}{\partial \bar{\theta}}(\sin(\pi\bar{\theta})\bar{u}_s)\right) + \pi^2\bar{u}_s\right], \quad (3)$$

where $\mathrm{Bo} = \gamma h_0/(\rho g \pi^2 R^3)$ is the Bond number, $A =
A'/6\pi\rho g R h_0^3$ is the dimensionless Hamaker constant,
and $\mathrm{Bq} = \varepsilon h_0/(\mu_{\mathrm{air}}\pi^2 R^2)$ is the Boussinesq number.
Terms on the right-hand side of (2) account, respectively,
for the hydrostatic, surface tension, and van der Waals
forces. The right-hand side of (3) represents the surface
shear viscous stress in the streamwise direction. The
system (1)–(3) is closed by imposing symmetric boundary
conditions at the poles,

$$\frac{\partial \bar{h}}{\partial \bar{\theta}} = \frac{\partial \bar{p}}{\partial \bar{\theta}} = \bar{u}_s = 0 \quad \text{at } \bar{\theta} = 0, 1. \quad (4)$$

Numerical simulations are performed using COMSOL®
with the aim to predict the antibubble lifetime as function
of the problem parameters. Given the wide dispersion of
experimental lifetimes, for which the standard deviation
can be as large as the mean value [10], we consider two
rupture scenarios (RSs). In the RS1 the antibubble dies
when the minimum film thickness $h_{\min}$ reaches a critical
thickness h_c (see, e.g., Ref. [11]), which can be due to the
presence of surface contaminant, electrostatic forces or
any other perturbative mechanism, like intermole-
cular forces. In the RS2 the antibubble dies when $h_{\min}$
gets to zero after the destabilization of the film due to
van der Waals forces. In either case, and due to drainage,
the rupture always occurs at the vicinity of the south pole.
As a reference case, we take for the computation, either
(RS1) $h_c = 100$ nm and $A' = 0$, or (RS2) $A' = 4 \times 10^{-20}$ J,
which is the theoretical value of the Hamaker constant
for a water-air-water system [4]. Note this value is identical
for an air-water-air system encountered in foams and
neither the presence of surfactants, nor their nature, are
expected to modify this value significantly [12]. Unless
specified otherwise, we also take $R = 1$ cm, $h_0 = 1$ μm,
and $\gamma = 30$ mN/m, which approximately correspond to
experimental conditions. These values give for the charac-
teristic drainage time $\tau = 186$ s and for the dimensionless
numbers $\mathrm{Bo} = 3 \times 10^{-7}$ and $A = 2.2 \times 10^{-5}$. Though the
Bond number is extremely small, surface tension cannot be
neglected if one wants to satisfy the symmetric boundary
conditions at the poles. As initial condition, we assume a
uniform film thickness, i.e., $\bar{h}(\bar{\theta}, 0) = 1$.

We first consider the no-slip condition at the air-liquid
interfaces, i.e., for $\mathrm{Bq} \to \infty$, and solve (1), (2), and (4) with
$\bar{u}_s = 0$. Numerical solutions are plotted in Fig. 3 at various
times $\bar{t}$ ranged from zero to the lifetime $\bar{t}_{\mathrm{life}} = 30.1$ reached
when $\bar{h}_{\min} = \bar{h}_c = 0.1$ (RS1). We observe that the air
accumulates at the north pole and forms a bulge as
observed experimentally (see Fig. 1). While the maximum
amplitude of the bulge increases more than a hundred
times, the radius of this bulge does not change significantly
with time. In the rest of the domain, the film remains nearly
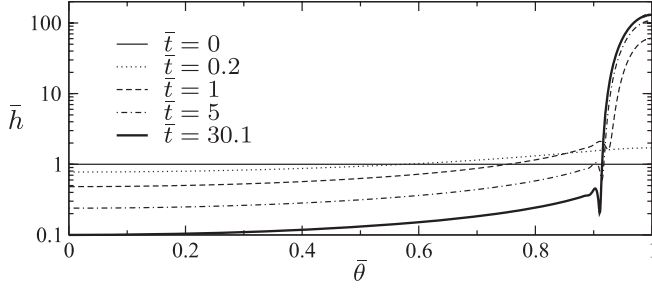flat. This is especially true at the south pole, where the film

FIG. 3. Time evolution of the antibubble film thickness with no-slip ($\bar{u}_s = 0$) and the first rupture scenario (RS1).

FIG. 5. Time evolution of the minimum film thickness for various surface shear viscosities, in the case of the RS2. The thick-dotted line separates the drainage period from the "instantaneous" rupture event. The numbers correspond to the slopes of the power-law behaviors.

thickness can then be assumed to be independent of position, i.e., $\bar{h} = \bar{h}_{min}(\bar{t})$ as $\bar{\theta} \to 0$. This assumption automatically implies that surface tension and van der Waals forces are neglected. It thus only applies for the RS1. Simplifying the system (1), (2), and (4) accordingly, and after some algebra, one gets the asymptotic behavior of the lifetime in the no-slip limit (see derivation in Ref. [8]):

$$t_{life}^{(RS1)} = \frac{3\mu_{air}R}{\rho g h_c^2}\left(1 - \frac{h_c^2}{h_0^2}\right) \quad \text{as Bq} \to \infty, \qquad (5)$$

which reduces to $t_{life}^{(RS1)} \approx 3\mu_{air}R/(\rho g h_c^2)$ for $h_c \ll h_0$, as predicted by Ref. [3]. This result shows that the antibubble lifetime is independent of the initial film thickness provided it is much larger than the critical thickness for rupture. This said, for our reference case, we get $t_{life}^{\infty} = 5660$ s, which is much above the values obtained in experiments, hence the central role of surface viscosity.

We now compute numerical solutions with the surface viscous model (1)–(4) and show in Fig. 4 the lifetime as a function of the surface shear viscosity for the two different rupture scenarios. In both cases, the lifetime increases with surface viscosity, though with different slopes, namely $t_{life} \propto \varepsilon$ for the RS1 and $t_{life} \propto \varepsilon^{5/6}$ for the RS2. One can show that the slope difference for the RS2 is due to the dependence of the critical thickness with the surface viscosity, as also found by Ref. [13] for bubble coalescence.
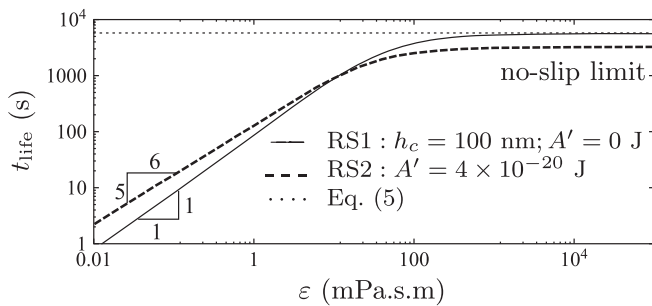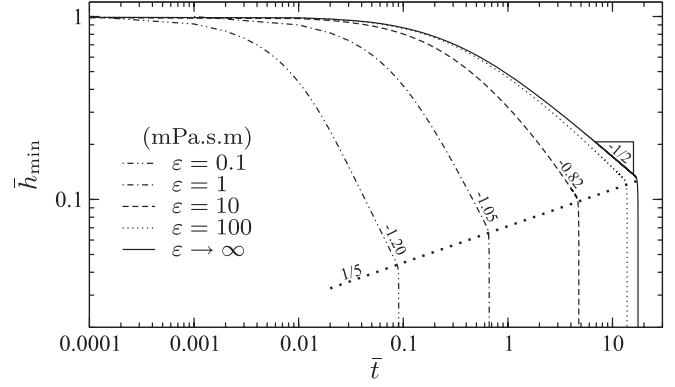
Figure 5 shows the time evolution of the minimum film thickness for various surface shear viscosities. As the minimum thickness decreases, it eventually reaches a power law until the film destabilizes due to van der Waals instability and breaks down on a time scale that is so short that we assume it is instantaneous. The exponent for the power-law behavior increases from $-1/2$ corresponding to the no-slip limit [see (5)] to values that approach the exponential behavior (not attainable with our model) corresponding to fully mobile interfaces [14]. The thick dotted line in Fig. 5 separates the drainage from the rupture. The slope gives the dependence between the critical film thickness and the lifetime as the surface viscosity is varied, i.e., $\bar{h}_c \propto \bar{t}_{life}^{1/5}$, hence $h_c \propto \varepsilon^{1/6}$ using the result in Fig. 4, which then shows the weak dependence of the critical thickness with the surface shear viscosity. Therefore, in the remainder of this Letter and for comparison with experiment, we only consider the RS2, which has the advantage to remove the arbitrary parameter h_c of the RS1, which was considered for general purpose and comparison with other theoretical results for critical thicknesses [11].
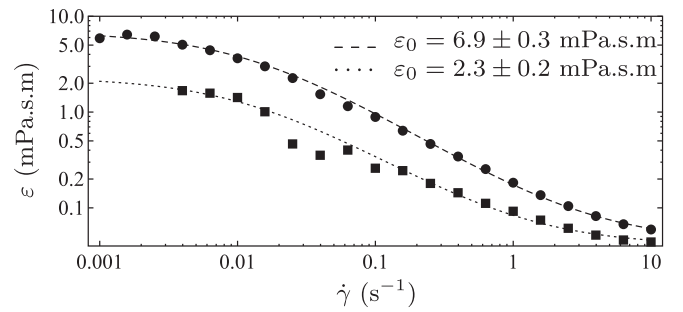

FIG. 4. Antibubble lifetime versus the surface shear viscosity for the two rupture scenarios. The dotted line corresponds to Eq. (5).

FIG. 6. Measurement of surface shear viscosity for varying shear rate $\dot{\gamma}$: (●) CAPB + SLES + MAC, (■) CAPB + SLES. The dotted and dashed lines are fits using the Cross model and where ε_0 is the value of the Newtonian plateau as $\dot{\gamma} \to 0$.

TABLE I. Theoretical and experimental results for antibubbles with $R = 5 \pm 2.5$ mm, $h_0 = 1$ μm and $A' = 4 \times 10^{-20}$ J (RS2).

	γ (mN/m)	τ_{ads} (s)	ε_0 (mPa$\cdot$s$\cdot$m)	$h_c^{(th)}$ (nm)	$t_{life}^{(th)}$ (s)	$t_{life}^{(exp)}$ (s)	Surfactant density at the interfaces
SLES + CAPB	28.5 [16]	$\sim 0.1^a$	2.3 ± 0.2	92 ± 6	487 ± 148	≈ 480 [10]	
SLES + CAPB + MAc	23.8 [16]	$\sim 3^a$	6.9 ± 0.3	110 ± 2	842 ± 66	≈ 750 [10]	Constant: $\tau_{ads} \ll \tau$
SDS (10*CMC)	36.7 [18]	~ 0.1 [19]	~ 0.001 [20]	21 ± 1	0.68 ± 0.32	<1 [10]	
$C_{12}E_6$ (10*CMC)	32.0 [21]	~ 100 [22]	<0.01	not applicable	not applicable	≈ 450 [3]	Non-constant: $\tau_{ads} \sim \tau$

^{a}Private communication with N. D. Denkov; see also Ref. [1].

We consider the experimental data by Dorbolo *et al.* [10] who used mixtures composed of 0.33 wt % SLES + 0.17 wt% CAPB (+ 0.02 wt% MAc) [15]. These mixtures have both a strong surface modulus and fast adsorption kinetics [16]. We have also measured the surface shear viscosities of these mixtures with an Anton Paar rheometer with the bicone method. Results are shown in Fig. 6 and depict a "shear thinning" behavior. The lines are fitted using the Cross model $\varepsilon = \varepsilon_\infty + \frac{\varepsilon_0 - \varepsilon_\infty}{1 + (C\dot{\gamma}^m)}$ [17], with the rate constant $m = 0.9$ and the consistency $C = 80$. The values of the Newtonian plateau for zero-shear rate are given in Fig. 6. Using $\varepsilon = \varepsilon_0$, consistently with the hypothesis of a "Newtonian" interface, we compute with our model the lifetime and the corresponding critical thickness at which the film destabilizes due to van der Waals interactions (RS2). The results are reported in Table I in terms of a mean value and a deviation based on the experimental radius dispersion, i.e., 5 ± 2.5 mm. The experimental lifetimes reported in Table I correspond to the largest values measured for each mixture in Ref. [10]. The longest lifetime corresponds to the thinnest critical film thickness whose value should thus be the closest to the critical film thickness triggered by van der Waals forces, which enables a comparison with our calculations. Actually, the theoretical and experimental lifetimes obtained this way are pretty close. Furthermore, whatever the critical thickness, i.e., whatever the probability for an antibubble to rupture at a given time, it is found that there is a factor of 2 between the experimental lifetime of an antibubble obtained with SLES + CAPB + MAc as compared to an antibubble obtained with SLES + CAPB. This factor 2 is fairly well recovered with our model, i.e., $842/487 \approx 1.7$. The fact that there are 2 orders of magnitude between the corresponding surface dilatational viscosities [16], excludes the possibility that dilational effects can rationalize the experimental observations of Ref. [10]. This conclusion is also supported by experiments on antibubbles with other surfactant mixtures as also reported in Table I. For instance, the great difficulty to generate antibubbles with sodium dodecyl sulfate (SDS) solutions is mentioned in Ref. [10]. Accordingly, surface shear viscosity for SDS solutions at concentrations much above the critical micelle concentration (CMC) is of the order of 10^{-3} mPa$\cdot$s$\cdot$m, which,

following our present model, gives lifetimes of the order of 0.68 ± 0.32 s, indeed too small to observe any antibubble experimentally. On the contrary, we succeeded in producing antibubbles with $C_{12}E_6$ [3], while the surface shear viscosity was measured to be below the limit of resolution of our surface shear rheometer, namely, <0.01 mPa$\cdot$s$\cdot$m. The explanation is that adsorption time for $C_{12}E_6$ is much larger than for the other surfactants reported in Table I such that the assumption of constant interfacial density of surfactant is not verified in this case.

All experiments on antibubbles report no dependence of the lifetime on the antibubble radius, while our model shows a nonmonotonic dependence: for small surface shear viscosity ε, the lifetime increases as the radius decreases while it is the contrary for large ε, in accordance with the no-slip limit Eq. (5). There should thus be a transition between these two limits for which the sensitivity of the lifetime to the radius is minimum. This is indeed observed from our simulation results reported in Table I for which the variation of lifetime with the radius is much smaller for SLES + CAPB + MAc than for SLES + CAPB. This observation, coupled with the stochastic behavior of film rupture, can explain why no radius dependence of the lifetime has yet been identified experimentally. Nevertheless, the present model assuming constant surfactant density at the surface allows us to rationalize the experimental data as summarized in Table I. This demonstrates that the surface viscosity can play a key role in delayed coalescence processes involving the drainage of an air film.

[1] J. Emile, A. Salonen, B. Dollet, and A. Saint-Jalmes, Langmuir **25**, 13 412 (2009).
[2] B. Scheid, J. Delacotte, B. Dollet, E. Rio, F. Restagno, E. van Nierop, I. Cantat, D. Langevin, and H. A. Stone, Europhys. Lett. **90**, 24 002 (2010).

[3] S. Dorbolo, E. Reyssat, N. Vandewalle, and D. Quéré, Europhys. Lett. **69**, 966 (2005).

[4] J. Israelachvili, *Intermolecular and Surface Forces* (Academic Press, Amsterdam, 2011), 3rd ed.

[5] J. Delacotte, L. Montel, F. Restagno, B. Scheid, B. Dollet, H. A. Stone, D. Langevin, and E. Rio, Langmuir **28**, 3821 (2012).

[6] F. Goodridge and I. D. Robb, Ind. Eng. Chem. Fundam. **4**, 49 (1965).

[7] P. G. Kim and J. Vogel, Colloids Surf. A **289**, 237 (2006).

[8] See Supplemental Material at http://link.aps.org/supplemental/10.1103/PhysRevLett.109.264502 for a detailed derivation of the model.

[9] J. C. Slattery, L. Sagis, and E.-S. Oh, *Interfacial Transport Phenomena* (Springer Verlag, Berlin, 2007), 2nd ed.

[10] S. Dorbolo, D. Terwagne, R. Delhalle, J. Dujardin, N. Huet, N. Vandewalle, and N. D. Denkov, Colloids Surf. A **365**, 43 (2010).

[11] E. D. Manev and A. V. Nguyen, Adv. Colloid Interface Sci. **114–115**, 133 (2005).

[12] N. D. Denkov, S. Tcholakova, K. Golemanov, and A. Lips, Phys. Rev. Lett. **103**, 118302 (2009).

[13] P.-S. Hahn and J. C. Slattery, AIChE J. **31**, 950 (1985).

[14] G. Debrégeas, P.-G. de Gennes, and F. Brochard-Wyart, Science **279**, 1704 (1998).

[15] SLES: sodium lauryl-dioxyethylene sulfate; CAPB: cocoamidopropyl betaine; MAc: myristic acid.

[16] K. Golemanov, N. D. Denkov, S. Tcholakova, M. Vethamuthu, and A. Lips, Langmuir **24**, 9956 (2008).

[17] M. M. Cross, J. Colloid Sci. **20**, 417 (1965).

[18] A. Q. Shen, B. Gleason, G. H. McKinley, and H. A. Stone, Phys. Fluids **14**, 4055 (2002).

[19] L.-H. Chen and Y.-L. Lee, AIChE J. **46**, 160 (2000).

[20] J. T. Petkov, K. D. Danov, and N. D. Denkov, Langmuir **12**, 2650 (1996).

[21] C. Stubenrauch, J. S. O. J. Rojas, and P. M. Claesson, Langmuir **20**, 4977 (2004).

[22] S.-Y. Lin, Y.-C. Lee, and M.-J. Shao, J. Chin. Inst. Chem. Eng. **33**, 631 (2002).